

12-19-2011

Aerosol-Assisted Synthesis of Monodisperse Single-Crystalline α -Cristobalite Nanospheres

Xingmao Jiang

Lihong Bao

Yung-Sung Cheng

Darren R. Dunphy

Xiaodong Li

University of South Carolina - Columbia, lixiao@cec.sc.edu

See next page for additional authors

Follow this and additional works at: https://scholarcommons.sc.edu/emec_facpub



Part of the [Applied Mechanics Commons](#), and the [Other Mechanical Engineering Commons](#)

Publication Info

Published in *Chemical Communications*, Volume 48, Issue 9, 2011, pages 1293-1295.

This Article is brought to you by the Mechanical Engineering, Department of at Scholar Commons. It has been accepted for inclusion in Faculty Publications by an authorized administrator of Scholar Commons. For more information, please contact digres@mailbox.sc.edu.

Author(s)

Xingmao Jiang, Lihong Bao, Yung-Sung Cheng, Darren R. Dunphy, Xiaodong Li, and C. Jeffrey Brinker

Cite this: *Chem. Commun.*, 2012, **48**, 1293–1295

www.rsc.org/chemcomm

COMMUNICATION

Aerosol-assisted synthesis of monodisperse single-crystalline α -cristobalite nanospheres†Xingmao Jiang,^{abc} Lihong Bao,^d Yung-Sung Cheng,^b Darren R. Dunphy,^c Xiaodong Li^d and C. Jeffrey Brinker^{*ce}

Received 15th September 2011, Accepted 15th November 2011

DOI: 10.1039/c1cc15713b

Monodisperse single-crystalline α -cristobalite nanospheres have been synthesized by hydrocarbon-pyrolysis-induced carbon deposition on amorphous silica aerosol nanoparticles, devitrification of the coated silica at high temperature, and subsequent carbon removal by oxidation. The nanosphere size can be well controlled by tuning the size of the colloidal silica precursor. Uniform, high-purity nanocrystalline α -cristobalite is important for catalysis, nanocomposites, advanced polishing, and understanding silica nanotoxicology.

Unlike the most abundant form of crystalline silica, α -quartz, which is trigonal and stable at temperatures below 573 °C, α -cristobalite is tetragonal in crystal structure (*P*41212 space group) and metastable at temperatures <270 °C at normal pressure.¹ Above 270 °C, α -cristobalite transforms into cubic β -cristobalite, but reconstructive transformation to quartz is kinetically limited. α -Cristobalite has a thermal expansion coefficient 4× greater than α -quartz, which makes it of interest for nanocomposites with enhanced mechanical, electrical, chemical, and thermal properties.² Compared with amorphous silica, crystalline α -cristobalite is a preferred catalytic material due to its high catalytic activity and selectivity for oxidative coupling of methane—especially with respect to the formation of ethylene.³ Due to its high surface reactivity, cristobalite has been claimed to be the most pathogenic polymorph of silica,⁴ and therefore synthesis of uniform, high-purity nanocrystalline α -cristobalite with controlled size is important for understanding the nanotoxicology of silicas.⁵ Many efforts have been made for synthesizing α -cristobalite, for example by annealing boiled

rice husks at high temperature.⁶ Hydrothermal methods^{7–11} employing amorphous silica as a starting material have been used, and result in tetragonal or cubic phases of cristobalite, respectively, when KF or NaF are used as the mineralization agents. However, for all these methods, based on cristobalite phase behavior, it has proven difficult to control cristobalite nucleation and crystal growth and therefore its size and morphology. Moreover, the crystalline silica particles¹² are often very large and severely aggregated. Synthesis of highly pure, nonaggregated, uniform single-crystalline nanospheres of the low-temperature polymorph, α -cristobalite, remains challenging.

Here we report a novel method for fabricating uniform, well-dispersed, highly pure α -cristobalite nanospheres. The process uses monodisperse silica colloids as precursors. The uniform monosized silica colloids with diameters ranging from ~5–300 nm were synthesized by a modified Stöber method.¹³ The colloids were dispersed as ~2–4% (wt) in ethanol or as 50–50 (v/v) in ethanol–hexane solution. The mixture was sprayed into aerosol droplets using a TSI 9302A atomizer with nitrogen as the carrier gas and a flow rate of 5 L min^{−1} using a method described previously.¹⁴ The aerosol dispersion was flowed into a horizontal ceramic tube furnace maintained at ~900–1100 °C. Under this high temperature, vapor pressure resulting from rapid evaporation/boiling of the solvent breaks up the aerosol and disperses the individual colloidal particles into a final, well-dispersed silica nanoparticle aerosol suspended in solvent vapor and nitrogen. A carbonaceous coating layer is deposited uniformly on each silica nanosphere to form a core–shell structured nanoparticle *via* accompanying chemical vapor deposition as a result of thermal decomposition of solvent molecules under the high temperature. Uniformly-sized carbon nanospheres were also generated by self-nucleation of the carbonaceous materials. Fig. 1 shows a representative TEM image of collected aerosol particles synthesized using ~280 nm colloidal silica particles as precursors. We observe a bimodal particle morphology composed of ~400 nm carbon-coated amorphous silica spheres and ~80 nm carbon nanospheres. TEM EDS elemental carbon mapping of the edges of the coated silica particles shows a uniform carbonaceous coating, which on average was ~60 nm thick. Thermal gravimetric analysis (Fig. S1, ESI†) showed a weight loss of 46.4% for oxidative pyrolysis of ~400 nm particles compared to 66.4% if the carbon shell were fully dense.

^a Key Laboratory of Fine Petrochemical Engineering, Changzhou University, Changzhou, 213164, PR China. Fax: +86-519-8633-0251; Tel: +86-519-8633-0253

^b Department of Chemical and Nuclear Engineering and Center for Micro-Engineered Materials, University of New Mexico, Albuquerque, NM 87131, USA. Fax: +1-505-272-7336; Tel: +1-505-272-7132

^c Aerosol and Respiratory Dosimetry Program, Lovelace Respiratory Research Institute, Albuquerque, NM 87108, USA. Fax: +1-505-348-8567; Tel: +1-505-348-9410

^d Department of Mechanical Engineering, University of South Columbia, SC 29208, USA. Fax: +1-803-777-0106; Tel: +1-803-777-8011

^e Sandia National Laboratories, MS1349, Albuquerque, NM 87106, USA. E-mail: cjbrink@sandia.gov; Fax: 01-505-272-7336; Tel: 01-505-272-7627

† Electronic supplementary information (ESI) available: TGA/DTA analysis of carbon coated silica particles. See DOI: 10.1039/c1cc15713b

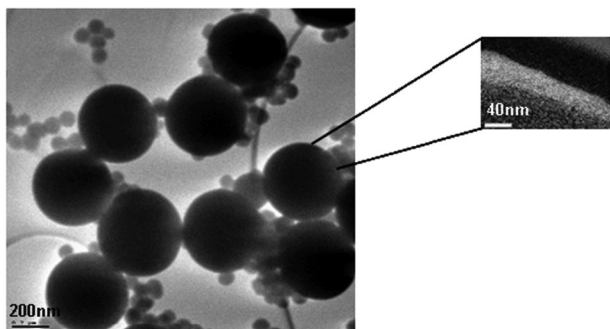


Fig. 1 TEM image for pyrolyzed carbon-coated amorphous silica nanoparticles. Scale bar: 200 nm. Inset shows a magnified view of the amorphous carbon coating (elemental mapping image), scale bar: 40 nm.

The smaller carbon nanospheres can be separated from the larger carbon-coated particles by centrifugation or gravity precipitation. The silica@C spheres were further calcined in inert gas at high temperature to devitrify the amorphous silica into crystalline silica.

Calcination of amorphous SiO_2 @C core/shell nanoparticles was performed in a horizontal alumina tube furnace. The furnace was sealed and heated to the desired temperature at a rate of $5\text{ }^\circ\text{C min}^{-1}$, and then held for the desired time to crystallize the amorphous SiO_2 @C core/shell nanoparticles. Highly pure Ar gas (99.99%) was introduced into the tube at a flow rate of $50\text{ cc (STP) min}^{-1}$ and the tube was kept at normal pressure or evacuated to a pressure of 4 Torr. The carbon on the particle surface was subsequently removed by wet oxidation *via* stirring in nitric acid or oxidatively pyrolyzed in air at $\sim 300\text{ }^\circ\text{C}$ for 5–30 h depending on carbon layer thickness and calcination conditions. The relatively lower temperature minimized the coarsening of the cristobalite spheres. Carbon content in the silica samples was checked by TGA/DTA analysis to confirm complete removal of carbon. Fig. 2 shows a representative TEM image for the $\sim 5\text{ nm}$ silica samples after calcination at $1100\text{ }^\circ\text{C}$ for 4 h followed by carbon removal, indicating that the silica nanospheres are monodisperse and that they preserve the size of

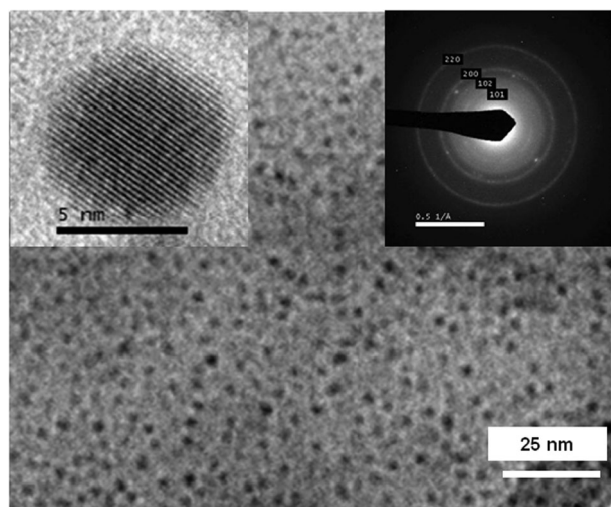


Fig. 2 TEM images for crystalline silica nanospheres after calcination at $1100\text{ }^\circ\text{C}$ and oxidation at $300\text{ }^\circ\text{C}$. Insets: HRTEM and SED. The crystallite size based on the Scherrer equation is 10 nm, assuming 0.9 for the shape factor.

the original colloidal silica precursors. Selected area electron diffraction of multiple nanospheres and a HRTEM of a single nanoparticle as shown in the insets of Fig. 2 jointly reveal that the silica nanospheres are single crystalline. The X-ray diffraction pattern shown in Fig. 3 indicates that the monodisperse silica nanospheres are pure phase α -cristobalite. The metastable low-temperature phase was formed by crystallization of β -cristobalite and its subsequent transformation into α -cristobalite upon cooling.

It is found that crystallization of the amorphous SiO_2 @C core/shell nanoparticles was dependent on the system temperature and pressure, and the size of the amorphous nanoparticles.¹⁵ For all the calcinations performed under atmospheric conditions (at ambient pressure) the calcined silica nanoparticles are still amorphous at temperatures of up to $1000\text{ }^\circ\text{C}$. However, when the calcination was performed under low pressure (4 Torr), the crystallization was observed to occur at as low as $750\text{ }^\circ\text{C}$ and well-crystallized cristobalite was formed at $800\text{ }^\circ\text{C}$. Fig. 4 shows the XRD patterns of the calcined nanoparticles of varying size and the corresponding crystallization temperatures. The lowest crystallization temperature increased with the size of nanoparticles. A low pressure is beneficial to nucleation and coarsening needed to achieve single crystal cristobalite during

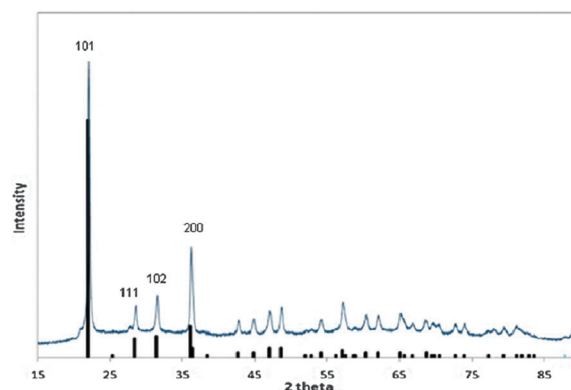


Fig. 3 XRD pattern for nanoparticles after treating 5 nm silica@C at $1100\text{ }^\circ\text{C}$ over 4 h. Standard diffraction peaks for α -cristobalite are marked for comparison.

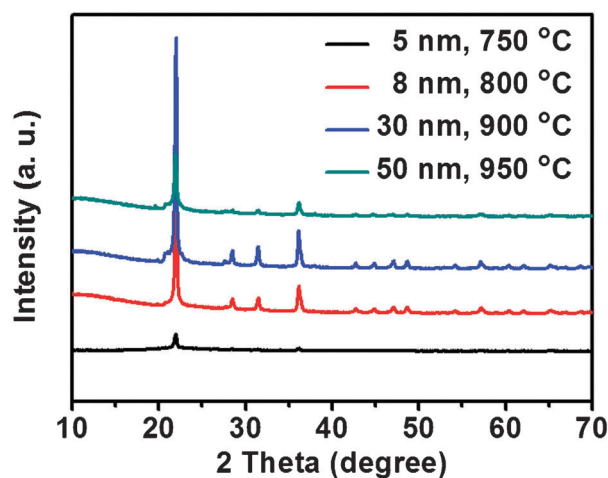


Fig. 4 XRD patterns of calcinated SiO_2 @C nanoparticles of different sizes.

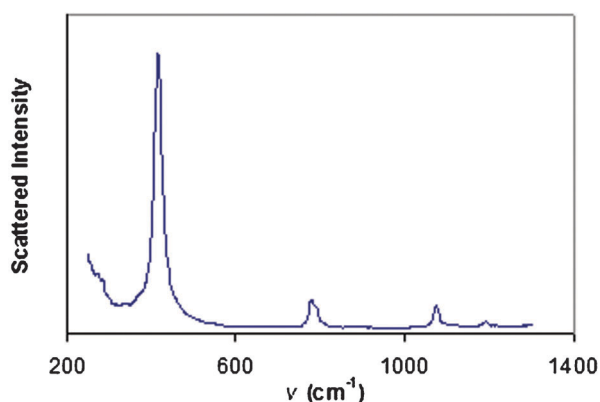


Fig. 5 Raman spectrum for cristobalite sample after treating 5 nm silica@C at 1100 °C over 4 h and oxidation at 300 °C.

devitrification.¹⁶ It may also be beneficial for evaporation of any impurities such as carbon and salts which would detrimentally affect nucleation and crystallization of cristobalite.¹⁷ At higher temperature (1400 °C), carbon will react further with silica to form SiC nanospheres or fused silica@SiC@C structures. A minimum thickness of the carbon shell is required to protect the silica core and block aggregation of silica nanospheres during high-temperature devitrification.

The Raman spectrum (Fig. 5) matches that of pure cristobalite.¹⁸ No peaks for carbon or amorphous silica were found, indicating that the sample has high purity and is fully crystallized. The size of cristobalite nanospheres is determined by that of the original Stöber silica colloidal precursors along with the greater relative density of cristobalite compared to amorphous Stöber silica, causing the final devitrified cristobalite nanoparticles to be smaller. To make uniform cristobalite nanospheres, the Stöber silica should be uniform in size. The obtained cristobalite can be used as grinding media, catalyst supports or as a filler in nanocomposites, and we expect this aerosol-assisted method to be generally useful for the fabrication of other uniform oxide nanospheres with controlled phase and size.

In summary, by using monodisperse amorphous Stöber silica nanoparticles as precursors and employing an aerosol assisted method to make amorphous SiO₂@C core/shell nanoparticles, thermal devitrification results in well dispersed, uniformly sized, single-crystalline α -cristobalite nanospheres. The method for high-quality cristobalite nanospheres is not only important for fillers, catalysts, and understanding silica nanotoxicology, but also provides a guideline for preparing other uniform crystalline nanospheres.

This work was supported by the National Science Foundation (EF-0830117 and CMMI-0968843), the National Institutes of

Health (U19 ES019528, UCLA Center for Nanobiology and Predictive Toxicology), the U.S. Department of Energy, Office of Science, Office of Basic Energy Sciences, Division of Materials Sciences and Engineering at Sandia National Laboratories and DOE BES grant DE-FG02-02-ER15368, the Army Research Office under Agreement/Grant W911NF-07-1-0320, and the Priority Academic Program Development of Jiangsu Higher Education Institutions. Sandia National Laboratories is a multi-program laboratory operated by Sandia Corporation, a wholly owned subsidiary of Lockheed Martin company, for the U.S. Department of Energy's National Nuclear Security Administration under contract DE-AC04-94AL85000.

Notes and references

- 1 http://www.quartzpage.de/gen_mod.html.
- 2 W. E. Zyl van, M. Garcia, B. A. G. Schrauwen, B. J. Kooi, J. Th. M. Hosson de and H. Verweij, Hybrid Polyamide/Silica Nanocomposites: Synthesis and Mechanical Testing, *Macromol. Mater. Eng.*, 2002, **287**(2), 106–110.
- 3 A. Palermo, J. P. H. Vazquez, A. F. Lee, M. S. Tikhov and R. M. Lambert, *J. Catal.*, 1998, **177**, 259.
- 4 B. Fubini, in *The Surface Properties of Silica*, ed. A. P. Legrand, Wiley, New York, 1998.
- 5 D. B. Warheit, T. R. Webb, V. L. Colvin, K. L. Reed and C. M. Sayes, *Toxicol. Sci.*, 2007, **95**, 270.
- 6 D. M. Ibrahim and M. Helmy, *Thermochim. Acta*, 1981, **45**(1), 79.
- 7 X. M. Jiang, Y. B. Jiang and C. J. Brinker, *Chem. Commun.*, 2011, **47**, 7524; J. F. Bertone, J. Cizeron, R. K. Wahi, J. K. Bosworth and V. L. Colvin, *Nano Lett.*, 2003, **3**, 655.
- 8 Y. Zhu, K. Yanagisawa, A. Onda and K. Kajiyoshi, *J. Mater.*, 2005, **40**, 3829.
- 9 B. Martin, *Eur. J. Mineral.*, 1995, **7**, 1389.
- 10 K. J. Lee, K. W. Seo, H. S. Yu and Y. I. Mok, *Korean J. Chem. Eng.*, 1996, **13**, 489.
- 11 E. N. Korytkova, L. F. Chepik, T. S. Mashchenko, I. A. Drozdova and V. V. Gusarov, *Inorg. Mater.*, 2002, **38**, 227.
- 12 M. Okabayashi, K. Miyazaki, T. Kono, M. Tanaka and Y. Toda, *Chem. Lett.*, 2005, **34**, 58.
- 13 W. Stober, A. Fink and E. Bohn, *J. Colloid Interface Sci.*, 1968, **26**, 62–69.
- 14 X. M. Jiang and C. J. Brinker, *J. Am. Chem. Soc.*, 2006, **128**, 4512.
- 15 S. K. Das, S. K. Mookerjee, S. K. Niyogi and R. L. Thakur, DTA study of kinetics of transformation of silica gel to cristobalite, *J. Therm. Anal. Calorim.*, 1976, **9**, 43–51; A. G. Verduch, *J. Am. Ceram. Soc.*, 1958, **41**, 427.
- 16 O. Yong-Taeg, S. Fujino and K. Morinaga, *Sci. Technol. Adv. Mater.*, 2002, **3**, 297–301.
- 17 H. Nanri, N. Takeuchi, S. Ishida, K. Watanabe and M. Wakamatsu, *J. Non-Cryst. Solids*, 1996, **203**, 375; N. Horii, M. Kamide, A. Inouye and N. Kuzuu, *J. Ceram. Soc. Jpn.*, 2010, **118**, 318; D. R. Bassett, E. A. Boucher and A. C. Zettlemoyer, *J. Mater. Sci.*, 1972, **7**, 1379; J. I. Corwin and A. C. Swinnerton, *J. Am. Chem. Soc.*, 1951, **73**, 3598.
- 18 D. C. Palmer, R. J. Hemley and C. T. Prewitt, *Phys. Chem. Miner.*, 1994, **21**(8), 481–488.